Supplementary text:

More detailed comparison of our modelling to borehole measurements, existing permafrost maps and local knowledge is presented here. Regional permafrost characteristics are also described. Additional figures and tables supporting the main text and the supplement can be found at the end of the supplement.

Russia

Our results can be compared to the MAGT at the ZAA on the Geocryological map of the USSR (scale 1:2,500,000, digitised to 100 m2 pixels) compiled in 1991 (Kondratieva et al., 1996), and representing several decades before the 2000-2016 period (Supplementary Figure 1). In the European part of Russia and northern part of Western Siberia (Yamal, Tazovsky and Gydan Peninsulas), the modelled mean MAGT appears overestimated by 2 to 4°C (Supplementary Figure 2). The sub-zero temperatures on the Kola Peninsula are not reflected by our mean MAGT, but are present in the ensemble spread. The permafrost extent seems to be overestimated in the Ob River floodplain, which is classified as wetland in the CCI landcover. The southern limits of permafrost are modelled too far north by 30-40 km at the Pechora River and 80 km in the area close to the Ural Mountains. MAGT in the Pechora Lowlands ranges from -0.5 to -2.5 °C (Malkova, 2010) and approaches 0°C in the Vorkuta region. The area is mainly underlain by discontinuous and sporadic permafrost. Our modelled MAGT in these areas is between 0.5 and -1 °C, and the modelled zones are sporadic and isolated patches. Numerous boreholes in these regions show both MAGT overestimation and underestimation by our model, with an average warm bias of 0.4 °C and SD of 1.2 °C. The continuous permafrost on the Pay-Khoy ridge and the coastal plain northwest of the Polar Urals (measured MAGTs between -2 and -3 °C) is modelled as discontinuous with MAGTs between -1 to 1.5 °C. The comparison to borehole data shows that modelled MAGT is underestimated by approx. 1 °C.

In the northern part of West Siberia, measured MAGTs range from -0.5 °C in regions with high shrubs and snow accumulation to -6 °C on snowless hilltops (Drozdov et al., 2010). The region (Yamal, Tazovsky and Gydan Peninsulas) is characterised by continuous permafrost with MAGT decreasing from -3 °C at a latitude of about 67°N to -6°C at 70°N, and -8°C on Bely Island. The ensemble mean of the modelled MAGT is warmer, with MAGT ranging from -2 to -2.5 °C at 67°N latitude, -3 to -4.5 °C at 70°N, and -5.5 °C on Bely Island. However, the SD of our model results exceeds 2°C in most of the region and measured MAGTs are therefore contained within the model ensemble. As a result of mean MAGT overestimation, the southern limit of permafrost is modelled about 100 km farther north in West-Siberian regions compared to the Geocryological map. However, there are sites with both positive and negative MAGT differences close to the southern limits of permafrost in this region.

The modelled MAGT is higher than borehole temperatures in some areas of northern East Siberia (mainly Taimyr) and both higher and lower in the southern parts. The areas at the southern permafrost limit show mostly MAGT overestimation so that the resulting permafrost limit is shifted about 500 km to the north-east, compared to the Geocryological map. Also in comparison to the Geocryological map, our modelled MAGT is considerably cold-biased (up to 5°C) in the central parts of East Siberia, which is confirmed by comparison to boreholes in the vicinity of Yakutsk showing an underestimation of MAGT by an average of 4 °C. This difference is at the limit or higher than the ensemble spread for this region, which is between 7 – 9 °C (SD of 2 – 2.5 °C) in forest-free areas and 3 – 4 °C (1 °C SD) in forested areas.

The modelled MAGT in the area between the Lena and Kolyma Rivers is within a reasonable interval of confidence for the tundra zone, but significantly underestimates south of the tree line. The modelled MAGT is also warmer (by 2 – 4°C) in the southern part of Far East Russia and colder in the northern part. Our modelled southern limit of permafrost is consequently shifted towards the north of Okhotsk Sea by 150 km compared to the Geocryological map. The model overestimates MAGT in the Amur region and Kamchatka by up to 3 °C according to the borehole data, which results in an underestimation of the permafrost area in this region by 50 % in comparison to the Geocryological map of the USSR. The extent of continuous permafrost in Eastern Siberia and Russian Far East is modelled realistically, except for the Chukotka and Magadan regions (North-East Russia), where it is underestimated.

Canada

Our modelled permafrost probability can be compared to detailed spatial modelling in southern Yukon Territory and northern British Columbia in western Canada (Bonnaventure et al., 2012) at 1 km^2 spatial resolution over a time period similar to this study's (post-2000). The permafrost probabilities obtained in the present study are generally lower south of 63.75°N, with a mean difference of -0.24 and greater (exceeding -0.5) over an extensive swath of the central southern Yukon where MAATs typically range from -3°C to -4°C (Lewkowicz et al., 2012). North of 63.75°N, the predictions are more similar, but low-elevation valley floors still feature lower probabilities in our map compared to Bonnaventure et al. (2012). Our permafrost probabilities are also compared to a permafrost map of Labrador and northern Québec (Way and Lewkowicz, 2016) (Supplementary Figure 5) at a 10 km2 spatial resolution for the period 1948-2014. There is a similar level of disagreement in this area as found for the southern Yukon Territory and northern British Columbia. The permafrost probabilities modelled in the present study are lower compared to Way and Lewkowicz (2016), especially south of 54°N (mean difference of -0.13), in the sporadic and extensive discontinuous permafrost zones in central Labrador and northern Québec between 55°N and 58°N, and also in the southern part of the continuous permafrost zone in Nunavik. Higher probabilities within our map were found at high elevations in the Torngat

Mountains. The substantial shift of permafrost zones northward on the eastern side of Hudson Bay is usually attributed to differences in snow cover thickness and duration (Burn, 2012),

China

Permafrost in China is mainly located in three regions in China: northeast China, the high mountains of western China, and the Tibetan Plateau. The permafrost distribution in northeastern It is mainly controlled by latitude, elevation and temperature inversions in low-lying areas. GlobPermafrost map was compared to Tibetan Plateau permafrost map using Kappa coefficients, which provide a measure for agreement between different probability classes (ranging from 0.50 to 0.95 with 0.05 intervals). The Kappa coefficients vary slightly between the classes, ranging from 0.66 to 0.76 (Supplementary Table 1)

Svalbard

The periglacial environment with permafrost underlies approximately 40 % (25 000 km2) of Svalbard (Humlum et al., 2003) from sea level to mountain tops. The permafrost there is typically about 100 m thick in the major valley bottoms, and up to about 400 - 500 m thick in the high mountains (Liestøl, 1976). The vicinity to the North Atlantic Current and the southern limit of polar pack ice makes Svalbard vulnerable to rapid climatic variations with potential effects on the permafrost (Humlum et al., 2003; Isaksen et al., 2007). Svalbard has undergone significant air temperature warming since 2000 (e.g. Hansen et al., 2014).

Greenland

The ice-free environment surrounding the Greenland Ice Sheet represents 20% (approximately 480 000 km2) of the area. The distribution of permafrost zones is primarily controlled by the overall climatic zonation from high arctic in the north to subarctic in the south, but is also influenced regionally by the climatic gradients from the coast to the Greenland Ice Sheet and over short distances, from valleys to mountain tops. Validation sites for permafrost zones, thickness and distribution are biased towards populated near-coastal locations in western Greenland and given these strong gradients, their representativeness is limited.

Permafrost zones in Greenland were mapped by Christiansen and Humlum (2000) and Westergaard-Nielsen et al. (2018) (Supplementary Figure 9). The first map is based on knowledge of local permafrost existence and the local air temperatures at meteorological stations. The latter map defines permafrost zones according to MAAT that is based on (1)

modelled atmospheric monthly mean temperatures from 1985 to 2015 at 1 and 5 km2 spatial resolution and (2) annual means of MODIS observed ground surface temperatures from 2001-2015.

Supplementary figures:

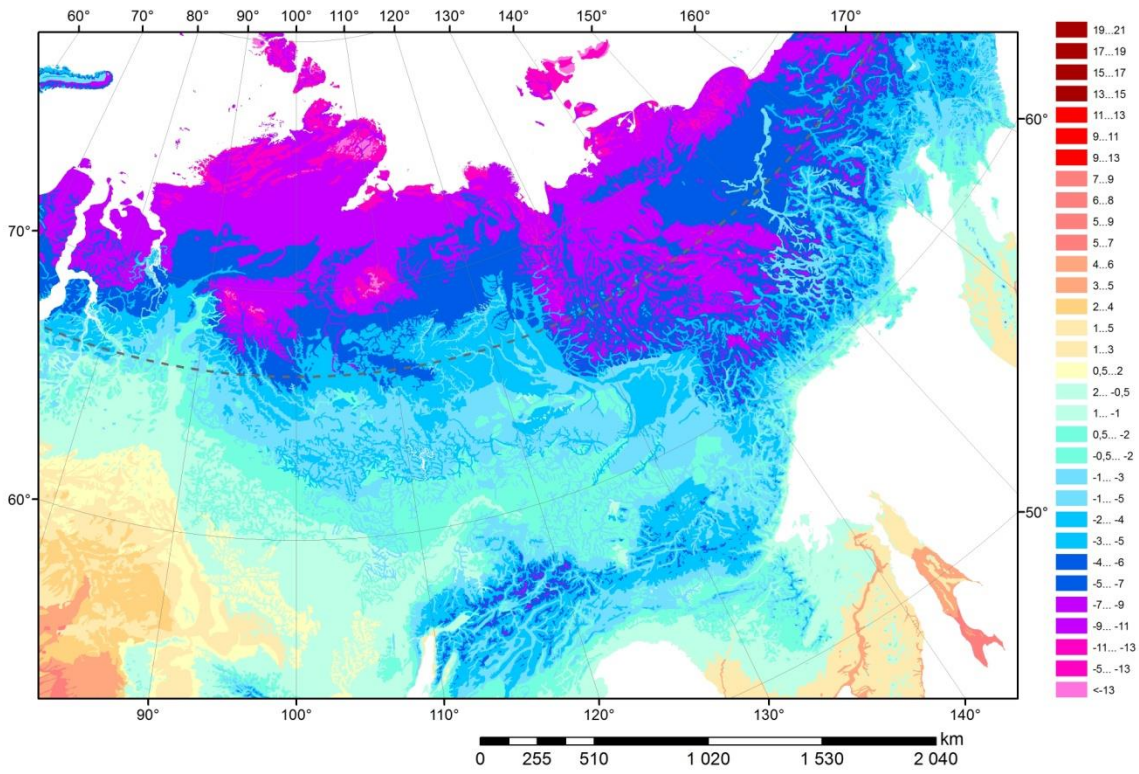

Supplementary Figure 1. Ground temperature layer of Geocryological map of the USSR as of 1991, showing MAGT at ZAA (Kondratieva et al., 1996).

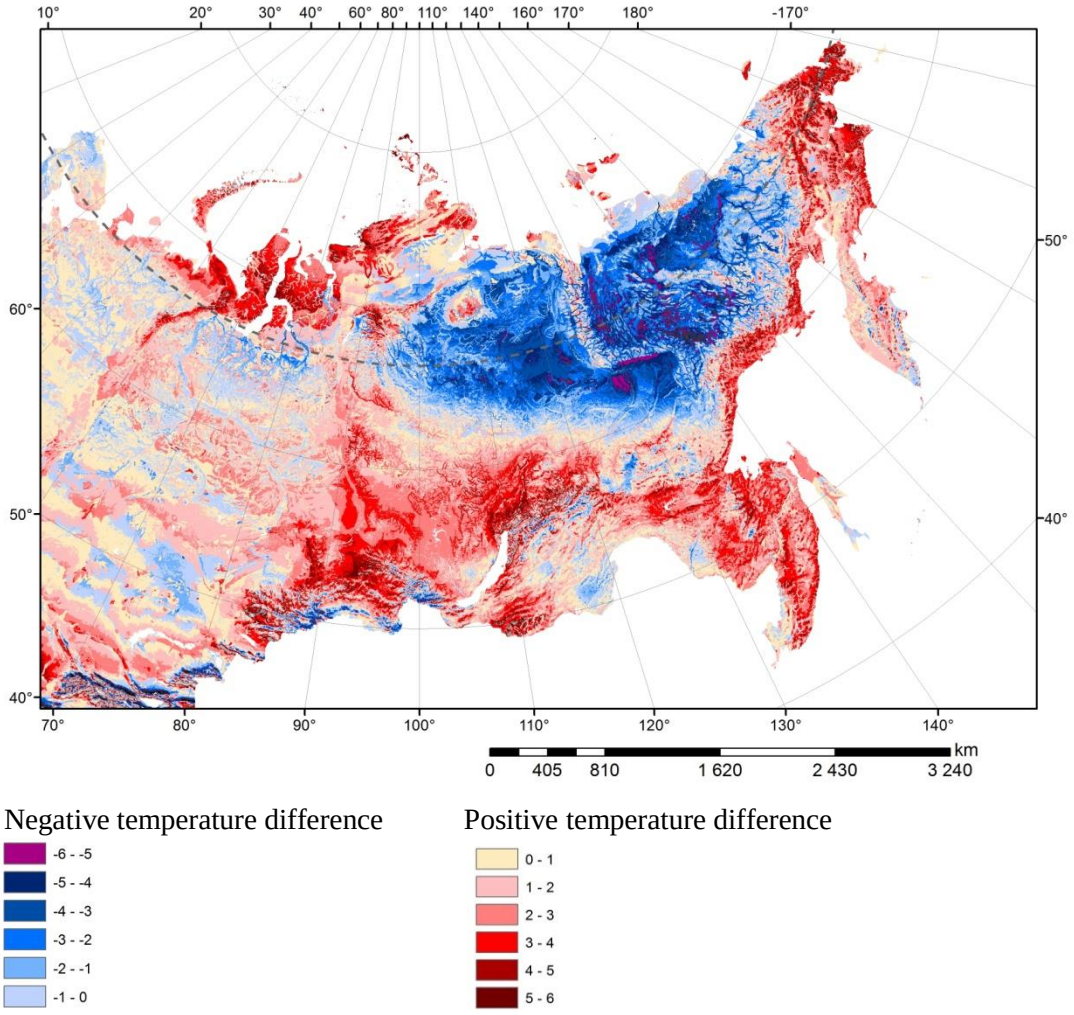

Supplementary Figure 2. Difference between ground temperature in Geocryological map of the USSR (at ZAA) and MAGT from GlobPermafrost map.

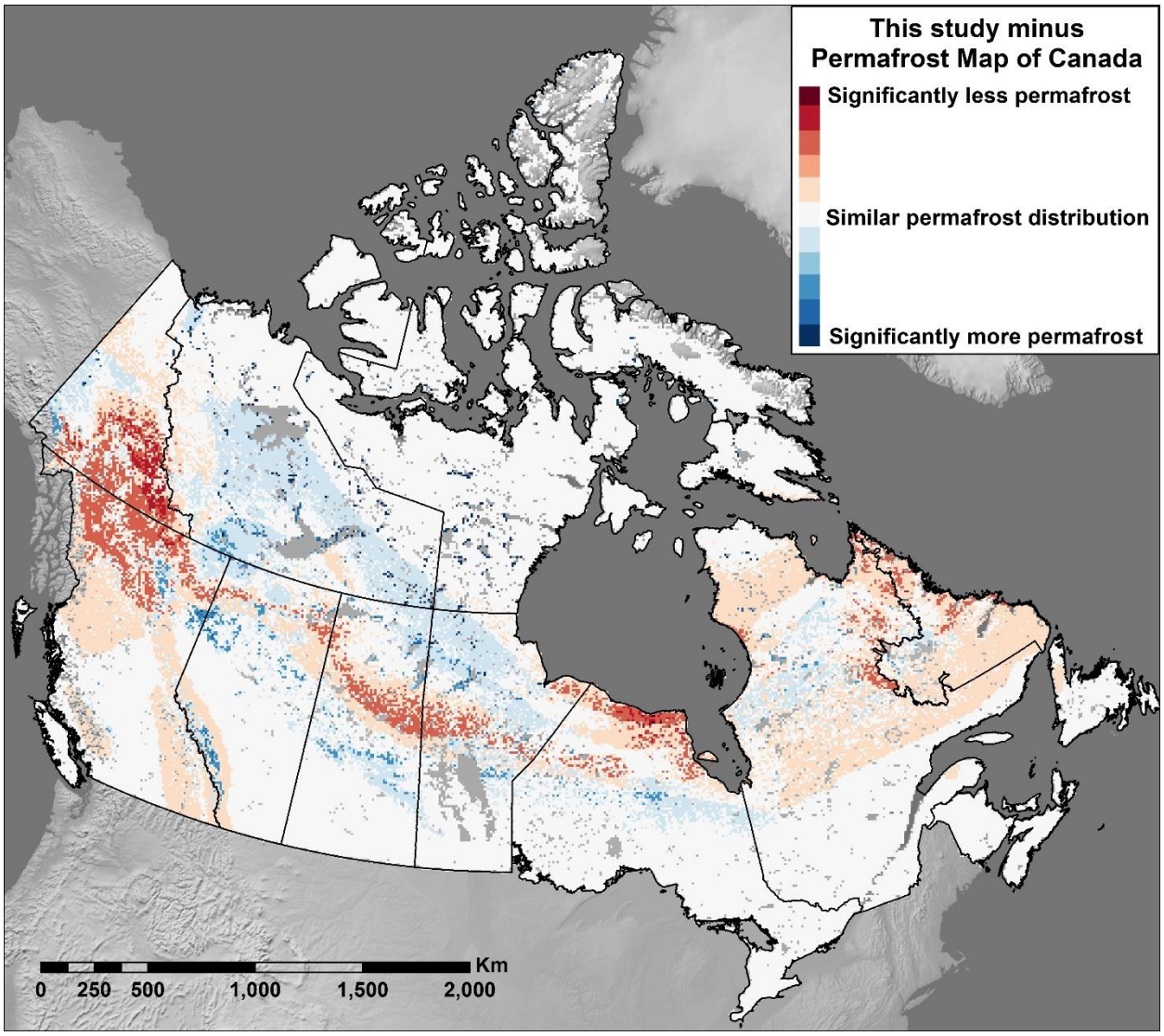

Supplementary Figure 3. Comparison between permafrost distribution from this study compared to the Permafrost Map of Canada derived from Heginbottom et al. 1995.

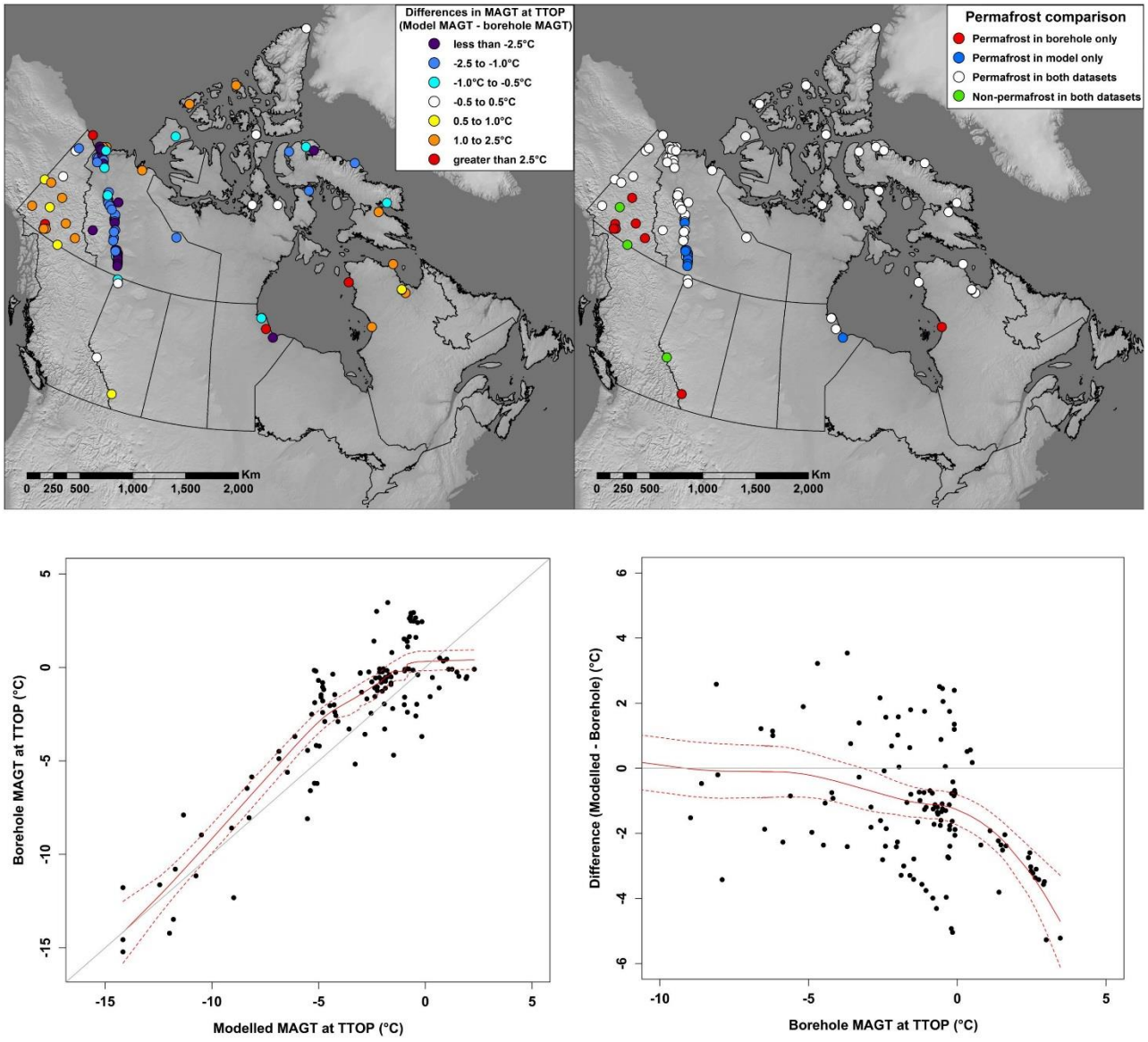

Supplementary Figure 4. Comparison between MAGTs modelled at borehole locations in Canada by this study and observed borehole MAGTs. (Top left) Mean differences between modelled MAGTs and borehole MAGTs. (Top right) Presence or absence of permafrost from modelled MAGTs and borehole MAGTs. (Bottom left) Scatterplot of modelled MAGTs and borehole MAGTs. 1:1 line is indicated in grey and locally weighted smoothing (span = 0.7) is shown in red with its respective upper and lower error limits. (Bottom right) Scatterplot of borehole MAGTs compared to the difference between modelled and measured borehole MAGTs. 1:1 line is indicated in grey and locally weighted smoothing (span = 0.7) is shown in red with its respective upper and lower error limits.

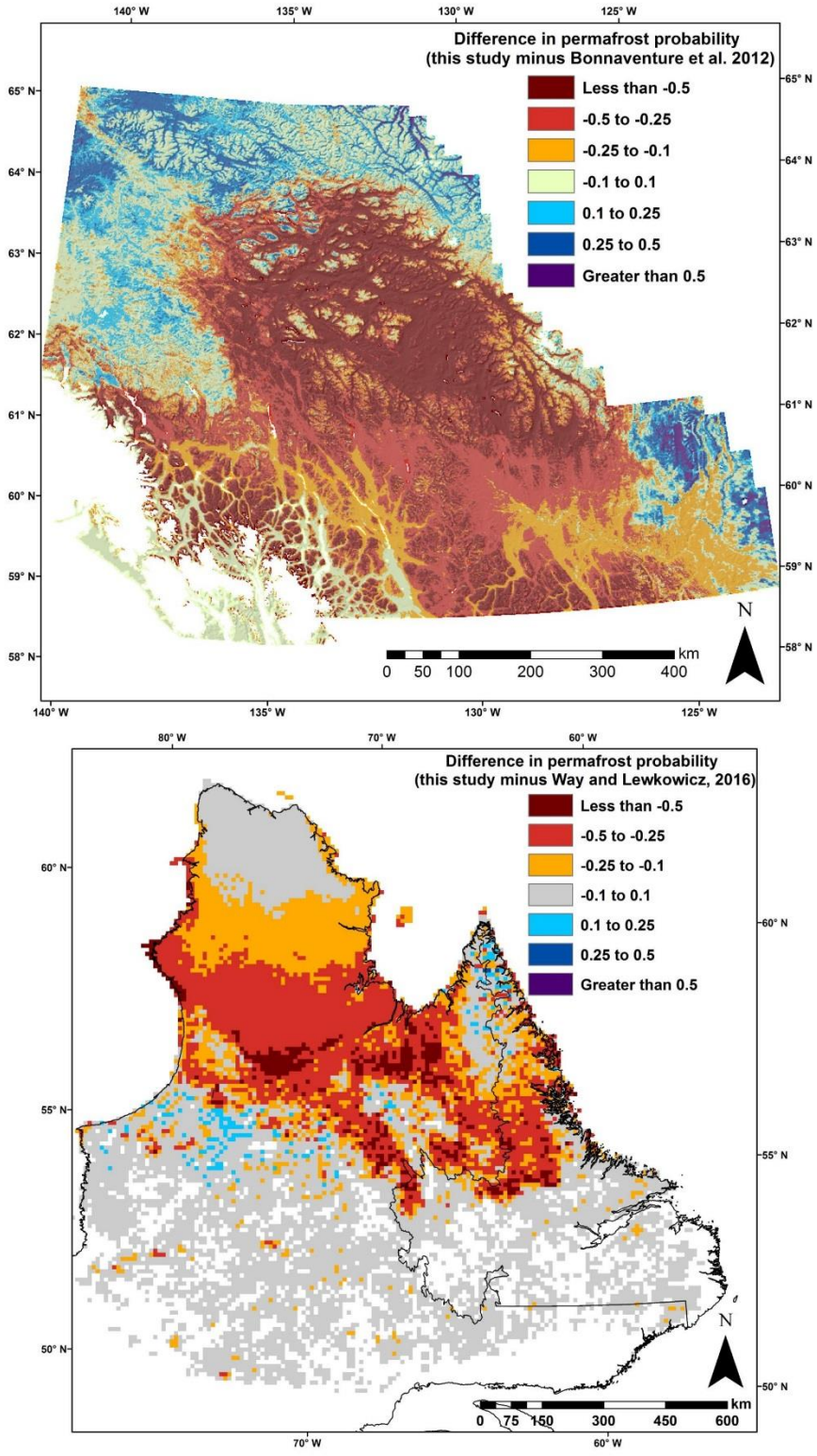

Supplementary Figure 5. Regional differences in permafrost probability between GlobPermafrost map and Bonnaventure et al (2012) for the southern Yukon, Canada and Way and Lewkowicz (2016) for Labrador-Ungava, Canada.

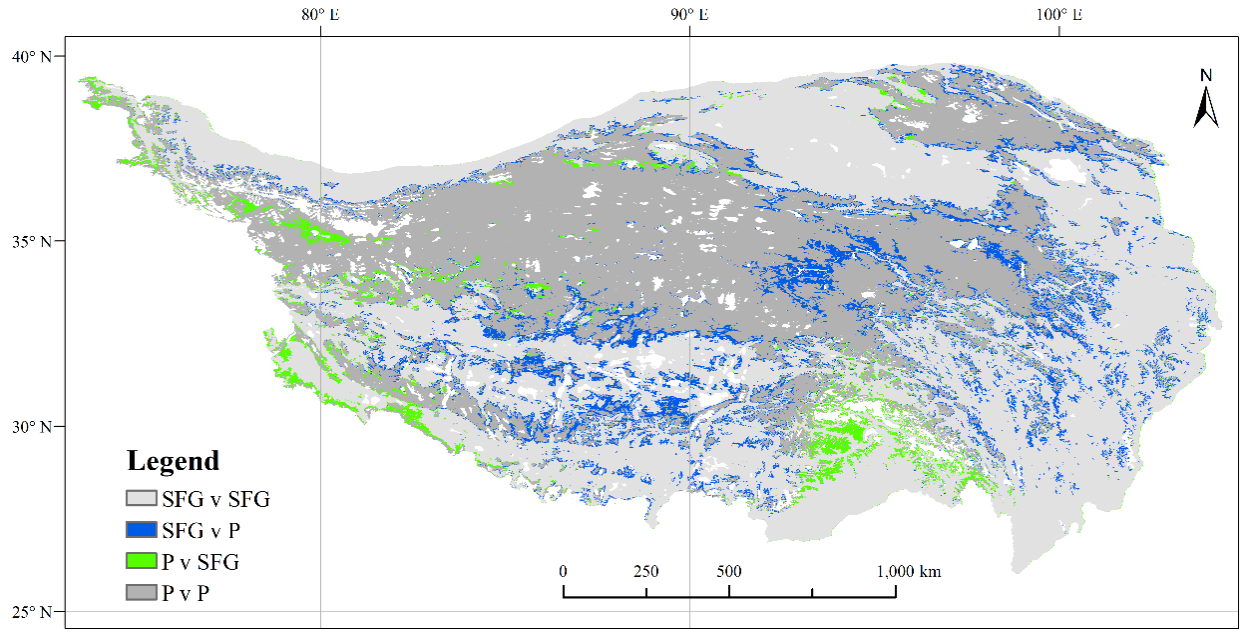

Supplementary Figure 6. Difference between GlobPermafrost map and Tibetan Plateau permafrost map (period 2003 – 2012) (Zou et al., 2017). Legend: SFG v SFG: seasonally frozen ground in both maps. P v SFG: permafrost in Tibetan Plateau permafrost map and seasonally frozen ground in GlobPermafrost map. SFG v P: seasonally frozen ground in Tibetan Plateau permafrost map and permafrost in GlobPermafrost map. P v P permafrost in both maps.

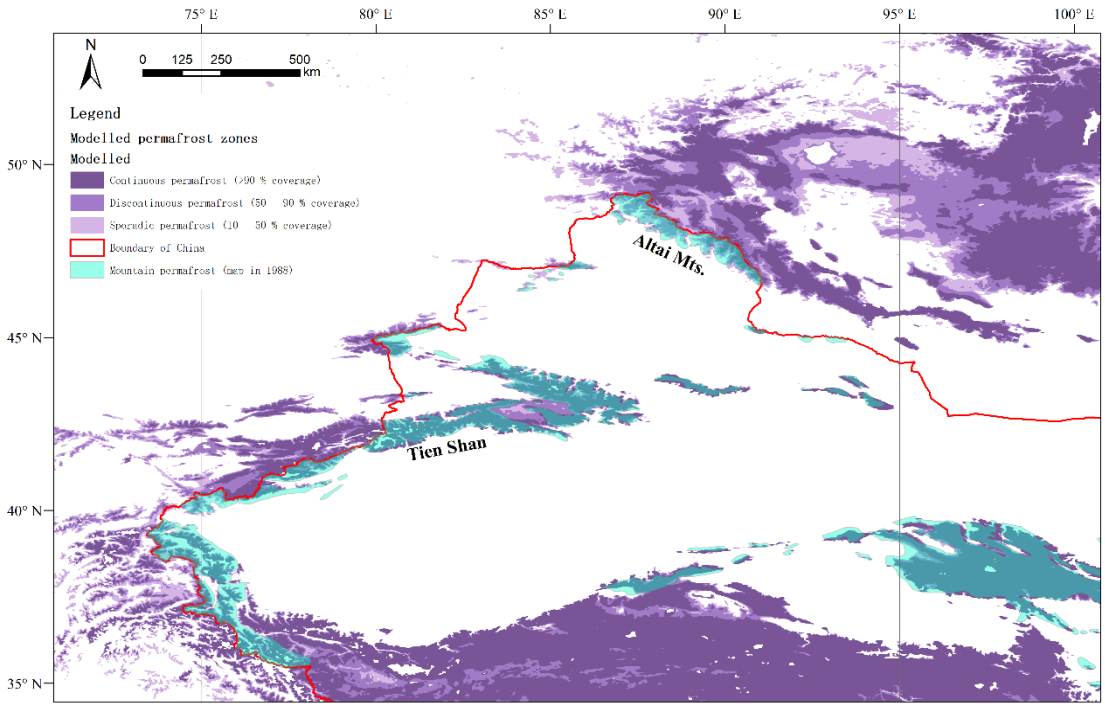

Supplementary Figure 7. Comparison of permafrost distribution in western China between the GlobPermafrost map and the Map of Snow, Ice and Frozen Ground in China (Shi et al., 1988).

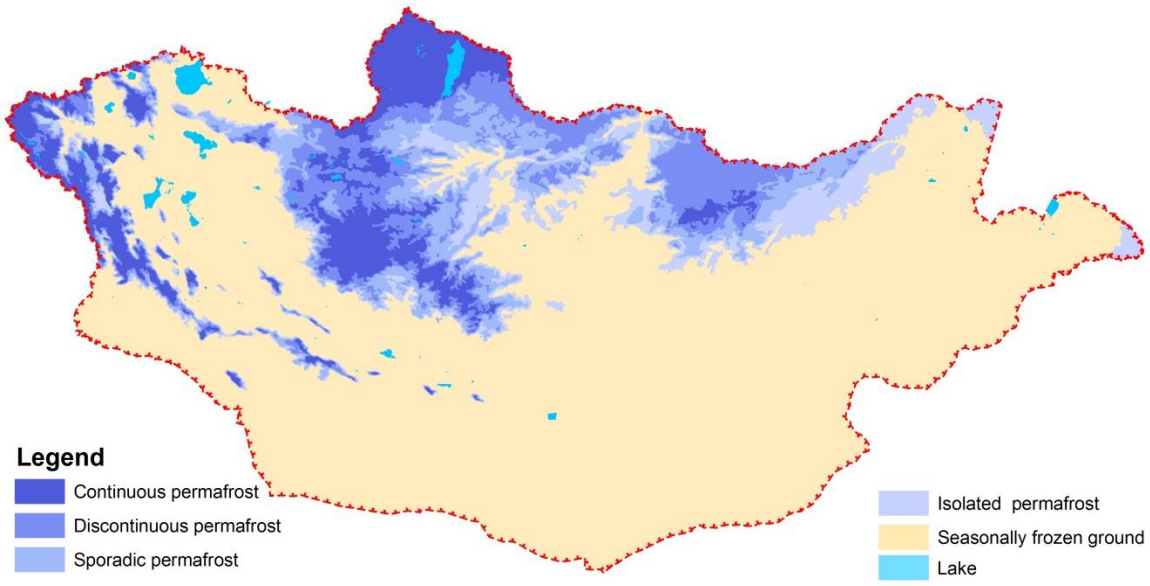

Supplementary Figure 8. Permafrost map of Mongolia by Jambaljav et al. (2017) showing temperature at the TTOP for the period between 2003 and 2013.

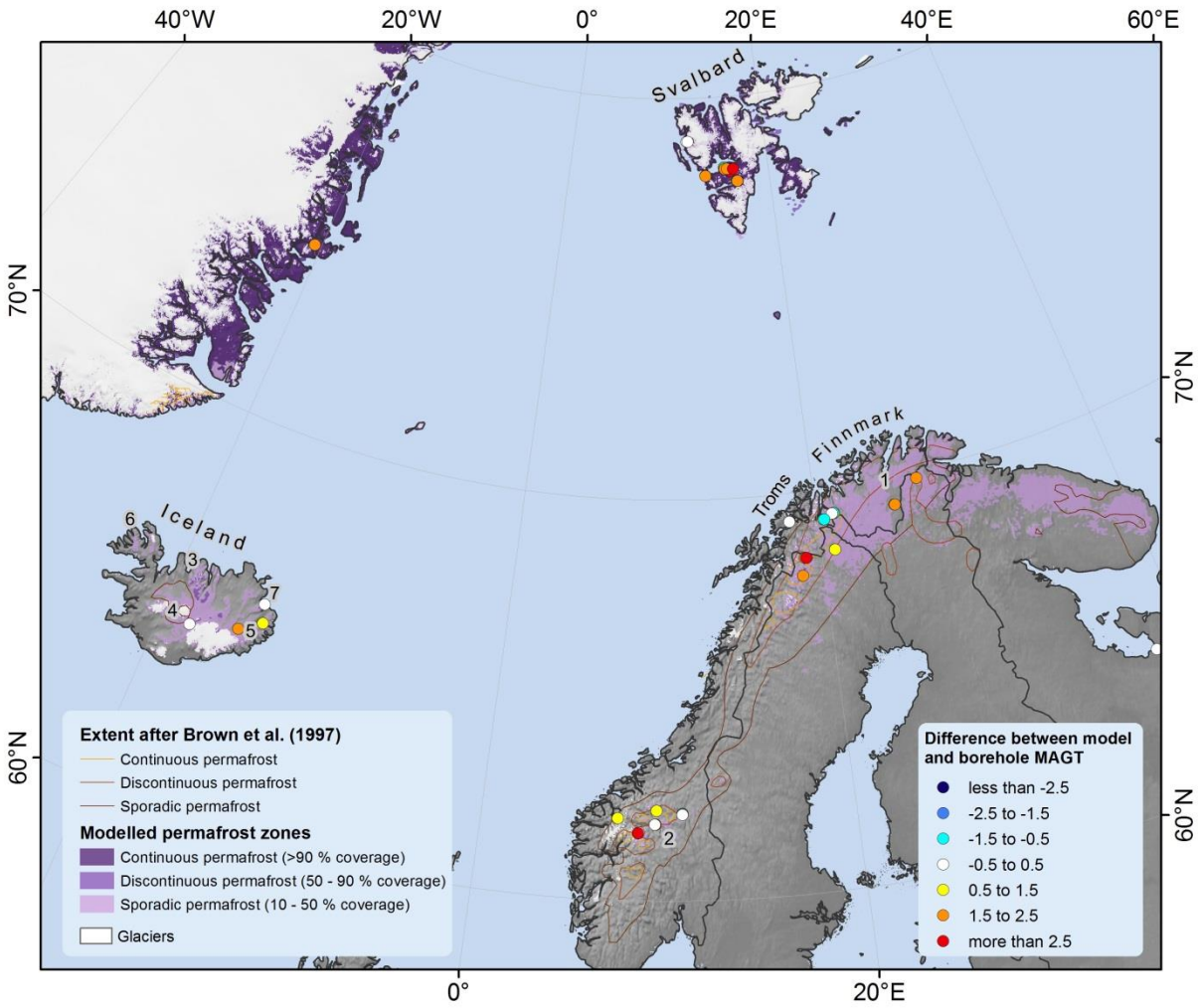

Supplementary Figure 9. GlobPermafrost zonation, permafrost extent after Brown et al. (1997) and difference between borehole and modelled MAGT for Scandinavia, Svalbard and Iceland. Note: isolated patches zone not shown. 1: Gaissane Mountains; 2: Rondane and Valdresflya; 3: Tröllaskági; 4: Hágöngur; 5: Egilsstaðir; 6: Vestfjord Peninsula; 7: Vopnafjörður.

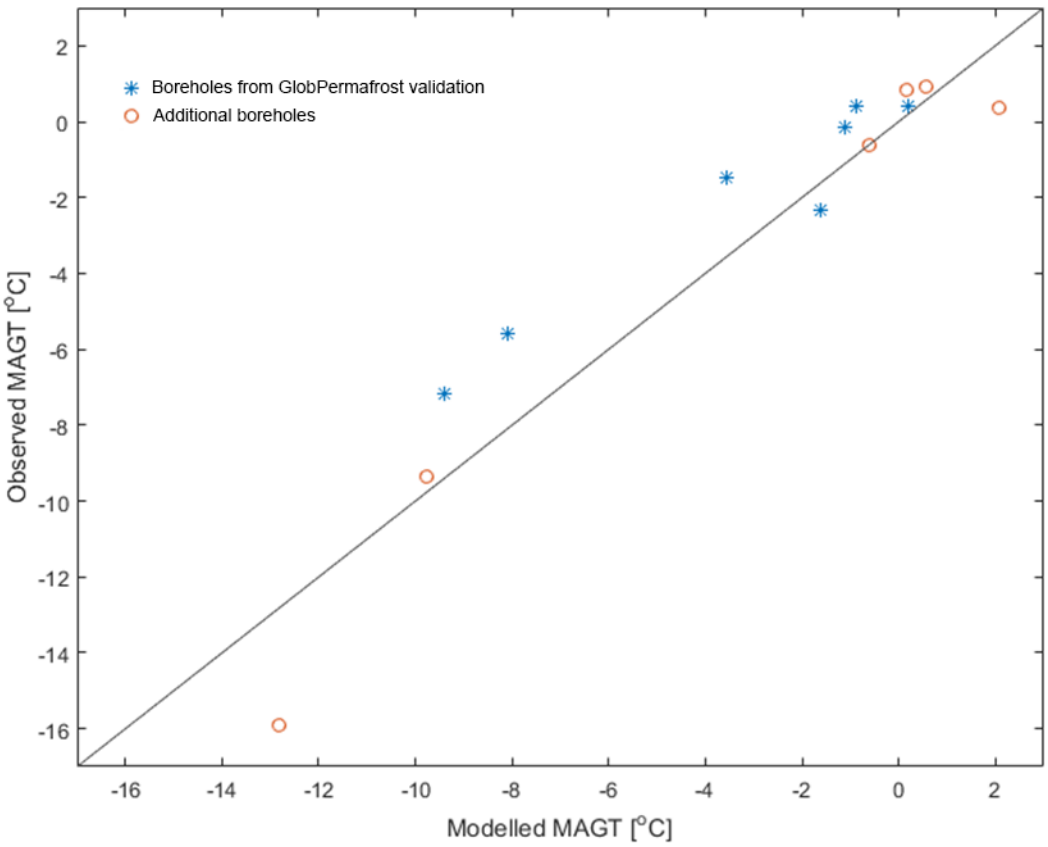

Supplementary Figure 10. Validation of the modelled MAGT in Greenland with additional six boreholes that were not included in the initial GlobPermafrost validation.

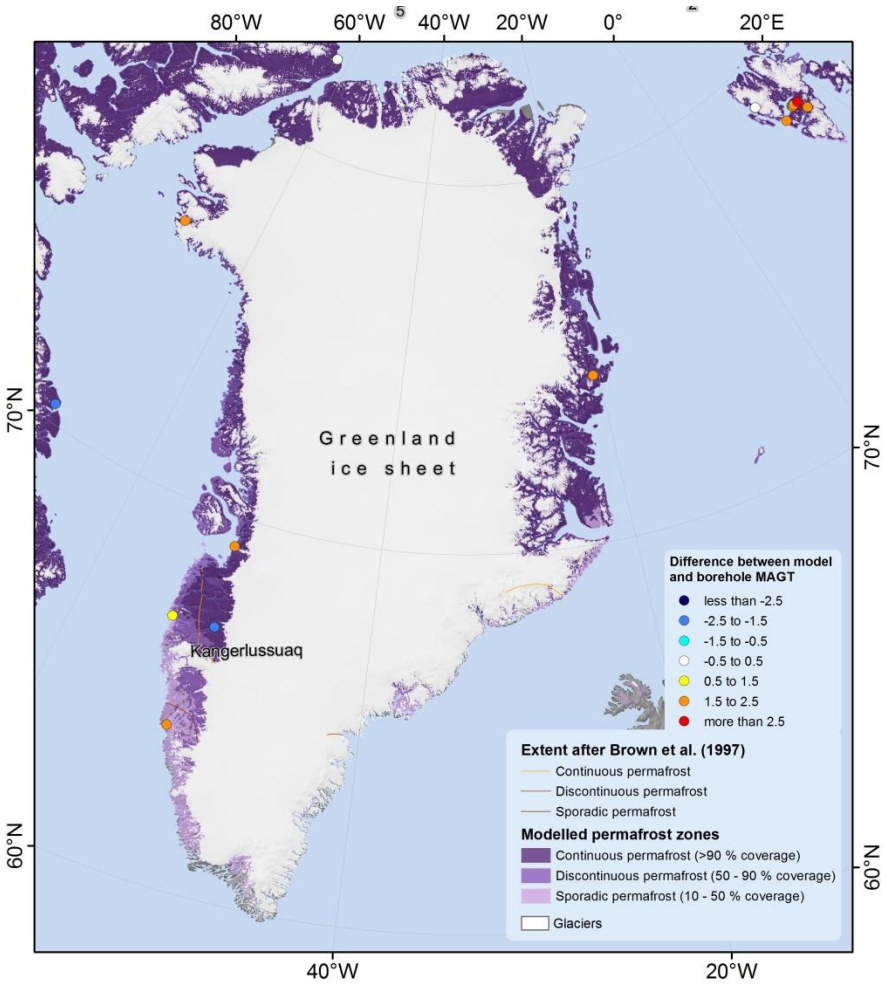

Supplementary Figure 11. GlobPermafrost zonation, permafrost extent after Brown et al. (1997) and difference between borehole and modelled MAGT for Greenland. Note: isolated patches zone not shown.

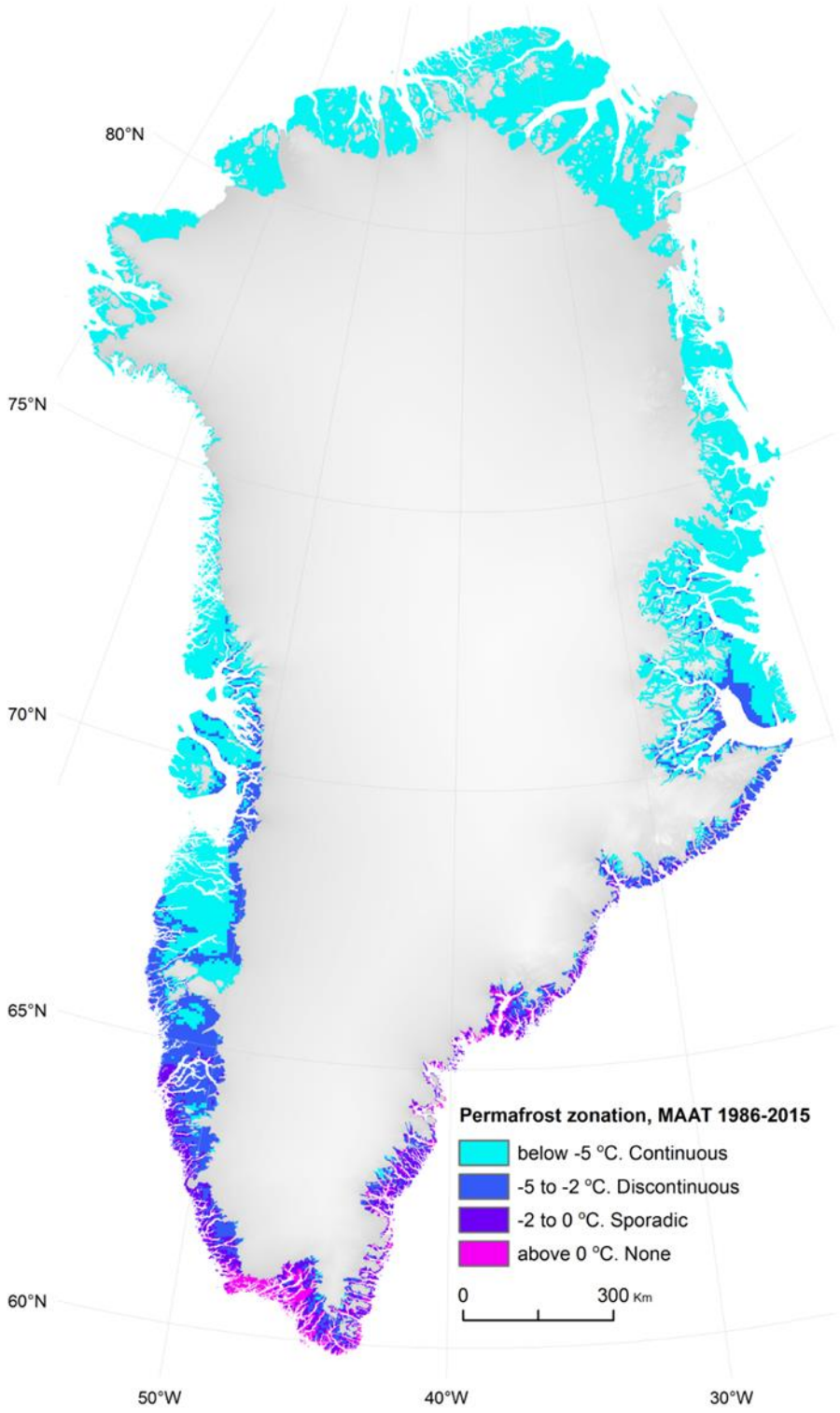

Supplementary Figure 12: General spatial distribution of permafrost types in ice-free Greenland. The classes are based on mean annual air temperatures (MAAT) from MAR v.3.5.2, covering the climate

normal 1986-2015. The 5 km spatial resolution captures general gradients from coast to inland, latitudinal, and east to west.

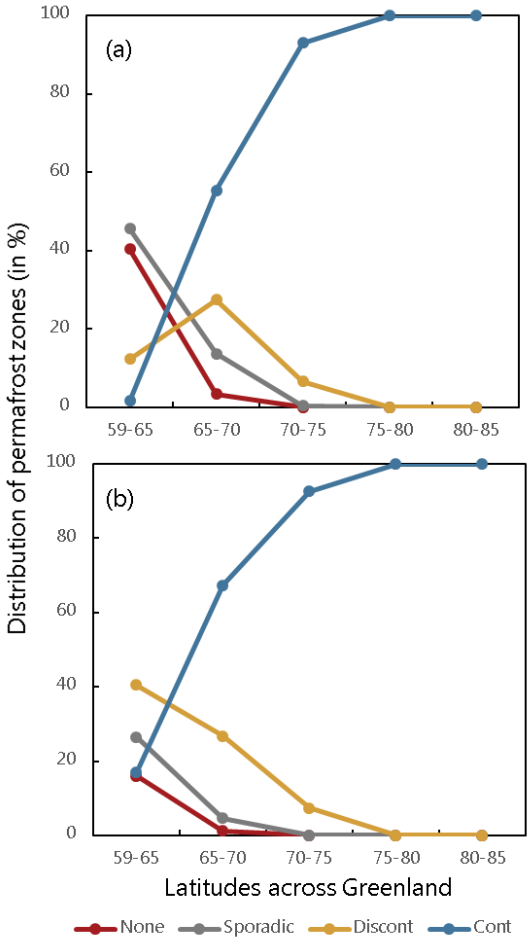

Supplementary Figure 13. The distribution (in %) of the four permafrost zones across five latitudes in Greenland: (a) is the new GlobPermafrost approach defined by modelled top permafrost temperatures, while (b) is the most recent published map (Westergaard-Nielsen et al, 2018) based on mean annual air temperatures (MAAT 1986-2015) at 1 and 5 km resolution (MAR data).

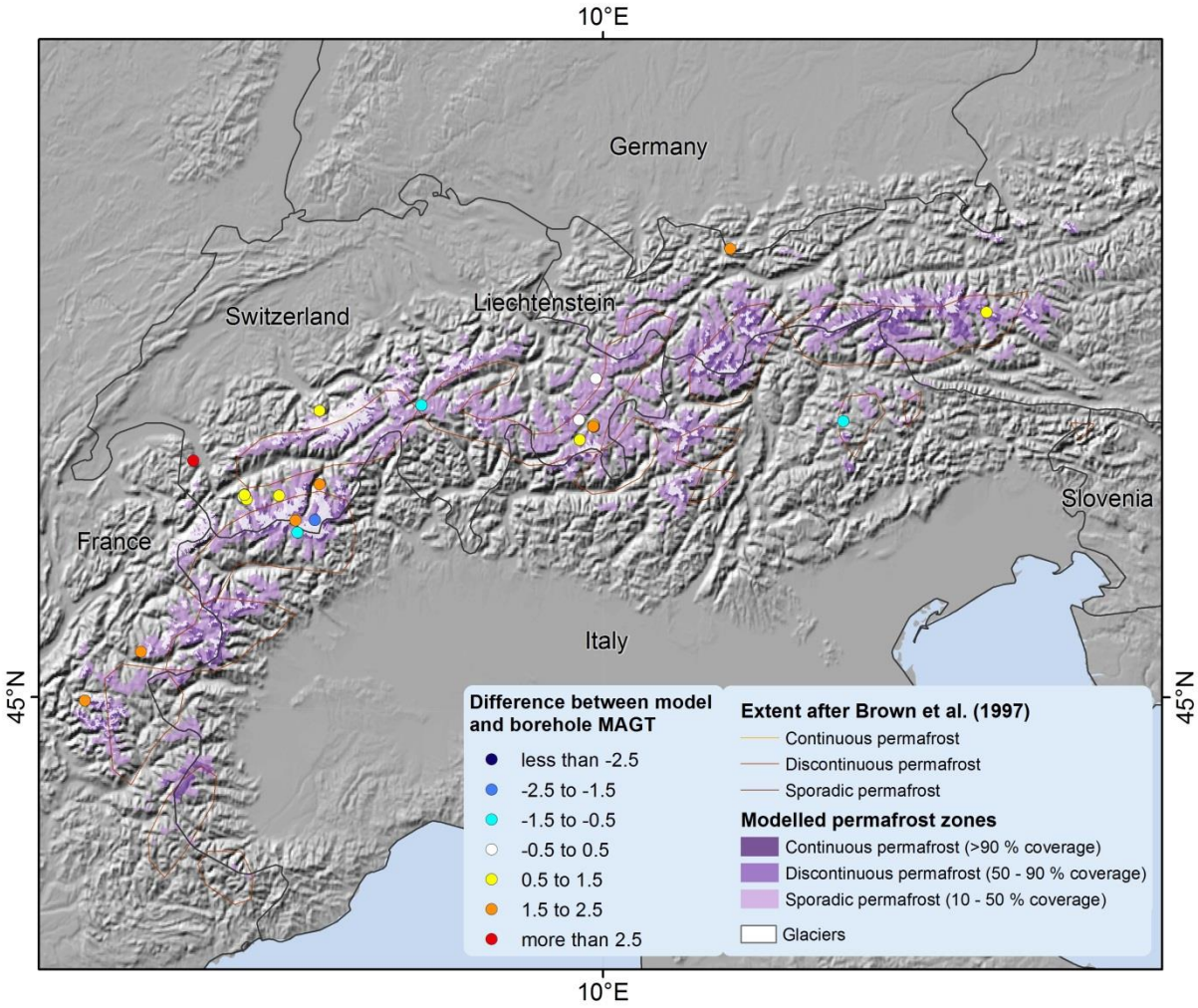

Supplementary Figure 14. GlobPermafrost zonation, permafrost extent after Brown et al. (1997) and difference between borehole and modelled MAGT for European Alps. Note: isolated patches zone not shown.

	Permafrost occurrence probability in fraction									
	0.50	0.55	0.60	0.65	0.70	0.75	0.80	0.85	0.90	0.95
Kappa coefficient	0.760	0.760	0.760	0.759	0.758	0.755	0.749	0.738	0.713	0.662

Supplementary Table 1. Kappa coefficients for different permafrost occurrence probability thresholds for comparison between our results and Tibetan Plateau permafrost map by (Zou et al., 2017)

References not cited in the main text:

Burn, C., 2011. Permafrost Distribution and Stability, in: French, H., Slaymaker, O. (Eds.), Changing Cold Environments. John Wiley & Sons, Ltd, pp. 126–146. https://doi.org/10.1002/9781119950172.ch7

Drozdov, D.S., Ukraintseva, N.G., Tsarev, A.M., Chekrygina, S.N., 2010. Change of permafrost temperature field and geosystem state on the urengoy oil-gas-field territory during the last 35 years (1974-2008). Kriosfera Zemli 14, 22–31.

Hansen, B.B., Isaksen, K., Benestad, R.E., Kohler, J., Pedersen, Å.Ø., Loe, L.E., Coulson, S.J., Larsen, J.O., Varpe, Ø., 2014. Warmer and wetter winters: characteristics and implications of an extreme weather event in the High Arctic. Environ. Res. Lett. 9, 114021. https://doi.org/10.1088/1748-9326/9/11/114021

Humlum, O., Instanes, A., Sollid, J.L., 2003. Permafrost in Svalbard: a review of research history, climatic background and engineering challenges. Polar Research 22, 191–215. https://doi.org/10.3402/polar.v22i2.6455

Isaksen, K., Benestad, R.E., Harris, C., Sollid, J.L., 2007. Recent extreme near-surface permafrost temperatures on Svalbard in relation to future climate scenarios. Geophysical Research Letters 34. https://doi.org/10.1029/2007GL031002

Lewkowicz, A.G., Bonnaventure, P.P., Smith, S.L., Kuntz, Z., 2012. Spatial and Thermal Characteristics of Mountain Permafrost, Northwest Canada. Geografiska Annaler: Series A, Physical Geography 94, 195–213. https://doi.org/10.1111/j.1468-0459.2012.00462.x

Liestøl, O., 1977. Pingos, springs, and permafrost in Spitsbergen. Norsk Polarinstitutt Arbok 1975, 7–29.

Malkova, G.V., 2010. Mean-annual ground temperature monitoring on the steady-state station '"Bolvansky."' Earth Cryosphere 14, 3–14.